

See discussions, stats, and author profiles for this publication at: <https://www.researchgate.net/publication/48446765>

Rapid Switching and High Contrast Electrochromic Property by Electrochemical Reduction of an Alternating Copolymer of Fluorene and Oxadiazole

ARTICLE *in* THE JOURNAL OF PHYSICAL CHEMISTRY C · MARCH 2010

Impact Factor: 4.77 · DOI: 10.1021/jp9108927

CITATIONS

3

READS

19

5 AUTHORS, INCLUDING:



Jianfu Ding

National Research Council Canada

142 PUBLICATIONS 5,238 CITATIONS

SEE PROFILE



Jianping Lu

National Research Council Canada

73 PUBLICATIONS 3,123 CITATIONS

SEE PROFILE



Hermenegildo Garcia

Technical University of Valencia

633 PUBLICATIONS 22,107 CITATIONS

SEE PROFILE



NRC Publications Archive (NPArc)
Archives des publications du CNRC (NPArc)

Rapid switching and high contrast electrochromic property by electrochemical reduction of an alternating copolymer of fluorene and oxadiazole

Ding, Jianfu; de Miguel, Maykel; Lu, Jianping; Tao, Ye; Garcia, Hermenegildo

Publisher's version / la version de l'éditeur:

Journal of Physical Chemistry C, 114, 11, pp. 5168-5173, 2010-01-03

Web page / page Web

<http://dx.doi.org/10.1021/jp9108927>

<http://nparc.cisti-icist.nrc-cnrc.gc.ca/npsi/ctrl?action=rtdoc&an=16124234&lang=en>

<http://nparc.cisti-icist.nrc-cnrc.gc.ca/npsi/ctrl?action=rtdoc&an=16124234&lang=fr>

Access and use of this website and the material on it are subject to the Terms and Conditions set forth at

http://nparc.cisti-icist.nrc-cnrc.gc.ca/npsi/jsp/nparc_cp.jsp?lang=en

READ THESE TERMS AND CONDITIONS CAREFULLY BEFORE USING THIS WEBSITE.

L'accès à ce site Web et l'utilisation de son contenu sont assujettis aux conditions présentées dans le site

http://nparc.cisti-icist.nrc-cnrc.gc.ca/npsi/jsp/nparc_cp.jsp?lang=fr

LISEZ CES CONDITIONS ATTENTIVEMENT AVANT D'UTILISER CE SITE WEB.

Contact us / Contactez nous: nparc.cisti@nrc-cnrc.gc.ca.



National Research
Council Canada

Conseil national
de recherches Canada

Canada

Rapid Switching and High Contrast Electrochromic Property by Electrochemical Reduction of an Alternating Copolymer of Fluorene and Oxadiazole

Jianfu Ding,^{*,†} Maykel de Miguel,[‡] Jianping Lu,[§] Ye Tao,[§] and Hermenegildo García[‡]

Institute for Chemical Process and Environmental Technology and Institute for Microstructural Science, National Research Council Canada, 1200 Montreal Road, Ottawa, Ontario, Canada, and Instituto Universitario de Tecnología Química, CSIC-UPV, and Departamento de Química, Universidad Politécnica de Valencia, Camino de Vera s/n, 46022, Valencia, Spain

Received: November 16, 2009; Revised Manuscript Received: January 31, 2010

While stable polymer electrochromic properties are mainly realized from the electrochemical oxidation of p-type conjugated polymers, in this paper we report that stable electrochromic properties can also be easily achieved by electrochemical reduction of n-type polymers, such as PF₄Ox, an alternating copolymer of quater(9,9-dioctylfluorene) and oxadiazole. The introduction of the strong electron-accepting oxadiazole unit into the poly(9,9-dioctylfluorene) main chain promoted the stability of the polymer in the electrochemical reduction. The copolymer film displayed an excellent electrochromic property upon electrochemical reduction, which turned the colorless film at the neutral state to rosy-red at the electron charged state with a switching time of 1.1 s. The film exhibited a high stability during the electrochromic test, having only 30% loss of the transmittance change in 500 potential square-wave cycles. Fourier transform infrared (FT-IR) study revealed that decay of the electrochromic performance of the film was associated with the formation of fluorenone and quinone defects on the fluorene unit in the copolymer chain. The laser flash photolysis test showed the monomer unit had a high potential to localize an electron and became highly vulnerable to be attacked by oxygen to form the defects. These defects would act as charge carrier traps and produced a pair of inner peaks at −1.84 and 1.03 V in the cyclic voltammetry test of the copolymer film.

Introduction

Electrochromic materials have the capability to reversibly change color when their oxidation states are converted by electrochemical means. These materials have received tremendous attention in recent years for many applications such as smart windows,¹ electrochromic displays,² and optic switches.³ Among several different types of electrochromic materials, conjugated polymers such as poly(3-alkylthiophene) and poly(3,4-alkylenedioxythiophene) derivatives have emerged with great potential in fabricating large area and flexible electrochromic devices.^{4,5} In addition, conjugated polymers have demonstrated good coloration efficiency, low operation voltage, short switching time, and high flexibility in color tuning.^{6–8} Though their electrochromic property can be realized by both electrochemical oxidation and reduction,^{1c} most of the applications rely on the electrochemical oxidation of electron-rich conjugated polymers such as derivatives of polythiophene, polytriphenylamine, and polycarbazole,^{4–7} due to higher charge mobility and higher stability of the oxidized state than the reduced state for most conjugated polymers. Only a limited number of materials have been reported to achieve color change based on electrochemical reduction.^{1c,8} On the other hand, most of the conjugated polymers reported for electrochromic applications have a narrow band gap and are often colored at the neutral state and bleached at the oxidized state. Unfortunately, the sharpness of the color

transition of this type of materials is lower than that of materials with a colorless neutral state.

Recently we observed that a very sharp color change can be easily achieved from a series of alternating copolymers of oligo(9,9-dioctylfluorene) and oxadiazole.⁹ As the copolymer film was reduced in an electrochemical cell, the color of the film turned from completely colorless to rosy-red. Their parent polymer, poly(9,9-dioctylfluorene) (PF), is a well-known electron-deficient polymer. It has been extensively studied for light-emitting diodes and showed certain instability upon annealing in air or under operation in light-emitting devices. It is believed that the instability is caused by the formation of a keto defect at the 9-carbon of fluorene under photo- or electrochemical conditions.^{10,11} List and Scherf¹¹ reported that the keto or fluorenone defects were easily formed in light-emitting devices at the electron charged state. Our previous research⁹ indicated that to introduce a strong electron-accepting unit, oxadiazole (Ox), into the PF main chain would be beneficial to stabilize the polymer at the electron-charged state. The alternating copolymers with the Ox unit evenly distributed in the PF chain with the Ox/F ratio varied from 1/2 to 1/4 exhibited much higher stability during annealing and the electrochemical reduction. Herein, the results of the electrochromic properties of the alternating copolymer of quater(9,9-dioctylfluorene) and oxadiazole (PF₄Ox) will be reported as an example, whose structure is illustrated in Scheme 1, and the degradation of the copolymer upon long-term electrochromic cycling will also be discussed.

Experimental Section

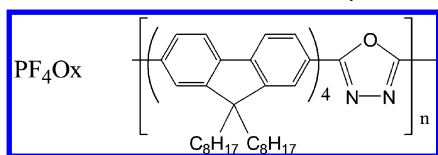
Materials. Toluene used for film preparation was purified by distillation over CaH₂. The synthesis and characterization

* Corresponding author: e-mail jianfu.ding@nrc-cnrc.gc.ca.

[†] Institute for Chemical Process and Environmental Technology, National Research Council Canada.

[‡] Universidad Politécnica de Valencia.

[§] Institute for Microstructural Science, National Research Council Canada.

SCHEME 1: Chemical Structure of PF₄Ox

of the copolymer PF₄Ox ($M_n = 30.4$ kDa, $M_w/M_n = 2.70$) used in this study has been reported previously.⁹

Physical Measurements. Cyclic voltammetry (CV) was performed in acetonitrile by use of a gastight three-electrode electrochemical cell on a Solartron SI 1287 potentiostat. Measurements were carried out at a scan rate of 50 mV/s at 20 °C under the protection of argon. A silver (Ag) wire was used as the quasi-reference electrode and a platinum (Pt) wire as the counterelectrode. A platinum disk (diameter 1 mm) sealed in a soft glass rod was employed as the working electrode. The testing film was prepared by casting a drop of the copolymer solution (8 mg/mL in toluene) on the disk electrode. Excess solution was removed by touching a piece of filter paper at the edge of the solution. Heating the sample at 80 °C for 2 min produced a thin uniform film on the working electrode, which was placed along with the counterelectrode and the quasi-reference electrode into the cell. The cell was then loaded with tetrabutylammonium hexafluorophosphate (Bu₄NPF₆, Fluka, electrochemical grade) and dried at 150 °C for 20 min under vacuum prior to being protected with argon. Five milliliters of acetonitrile (HPLC-grade, dried with CaH₂) was then distilled into the cell under vacuum to produce a 0.1 M Bu₄NPF₆ solution. The CV curves were recorded by scanning the potentials versus the Ag quasi-reference electrode, which was calibrated by the use of the ferrocene/ferrocenium redox couple. The electrochromic test was done by integrating a Solartron SI 1287 potentiostat and a Hewlett-Packard 8453 UV-vis spectrometer. The electrochemical cell used for this test had a similar configuration with the cell for CV test, except for a gastight UV curvature used as the cell and an ITO-coated glass strip (15 Ω/square, 5 × 30 mm²) used as the working electrode. The copolymer was dip-coated onto the working electrode from a toluene solution (20 mg/mL). The testing was done by applying potential step scans or potential square-wave cycles on the copolymer film. Laser flash photolysis experiments were carried out in a Luzchem nanosecond laser flash system using a dye laser (355 nm) for excitation (pulse ≤ 10 ns) and a 175 W ceramic xenon fiber-optic light source, Cermax, perpendicular to the laser beam as a probing light. The signal from the monochromator/photomultiplier detection system was captured by a Tektronix TDS 3032B digitizer. Laser system and digitizer were connected to a PC computer via general purpose interface bus (GPIB) and serial interfaces that controlled all the experimental parameters and provided suitable processing and data storage capabilities. The software package were developed in the LabView environment from National Instruments and compiled as a stand-alone application. The sample in a Suprasil quartz 0.7 × 0.7 cuvette capped with septa was purged with a N₂ or O₂ flow for at least 15 min before laser experiments. Microscopic images were taken on a Leica DM RD automatic photomicro system under a reflection mode using QCapture Pro 6.0 software.

Results and Discussion

1. Electrochromic Properties of PF₄Ox. As shown in Figure 1, the PF₄Ox film exhibits stable cyclic voltammograms (CV) with highly reversible n-doping and p-doping processes. When

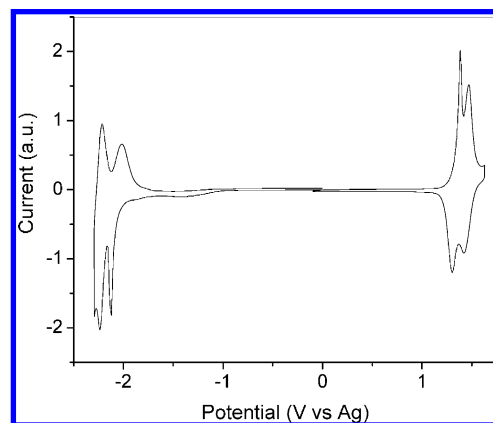


Figure 1. Cyclic voltammograms of PF₄Ox film, which was prepared by drop-coating a toluene solution on the Pt disk electrode, and the CV was recorded in 0.1 M Bu₄NPF₆ solution of CH₃CN at a scan rate of 50 mV/s. The potentials are measured relative to an Ag wire quasi-reference electrode.

the film on Pt working electrode underwent n-doping and p-doping processes separately, the CV curves did not have notable change in 10 cycles, indicating high stability of the copolymer under CV scanning conditions. Both the reduction and oxidation processes of the films contained two redox couples with half-wave potentials of −2.06 and −2.22 V for reduction and 1.34 and 1.45 V for oxidation. The redox couples at −2.22 and 1.34 V are at similar positions as those of PF.^{9b} Therefore, they can be attributed to electron and hole injection into the fluorene segment, respectively, while the other two redox couples at −2.06 and 1.45 V are associated with electron and hole injection into the Ox-containing segment. Due to the strong electron-withdrawing property of the Ox unit, the segment containing an Ox unit can be reduced at a less negative potential but can only be oxidized at a more positive potential. The band gap of the copolymer can be estimated from the difference of the onset potentials of reduction and oxidation processes, being 3.05 eV. This value is lower than that of the parent polymer, PF, which is 3.33 eV measured under the same conditions.^{9b} The decrease of the band gap of the copolymer is due to the existence of the Ox unit in the main chain. Its strong electron-withdrawing property reduces the lowest unoccupied molecular orbital (LUMO) level from −2.25 to −2.49 eV, while the highest occupied molecular orbital (HOMO) level remains nearly unchanged (5.58 vs 5.54 eV).

When the film was charged with electrons in the n-doping process, the film apparently turned from transparent to rosyr-red and then returned completely to transparent when the electron dedoping was completed. Its electrochromic property was further studied by the means of electrochromic absorbance spectra with a potential step scan on the copolymer film coated on an ITO electrode (5 × 25 mm² of coating area) via a combination of a potentiostat and an UV-vis spectrometer. In this case, a three-electrode configuration was still used for applying potential to the copolymer film. During the test, the electrochromic absorbance spectra were recorded. Figure 2 represents a typical result.

When the potential was −0.5 V, the copolymer was at the neutral state, where the film had a strong absorption peak in UV region with a peak centered at 380 nm. It did not show any absorption in the visible region. As the film was charged with electrons at −1.95 V, the intensity of the peak in the UV region decreased significantly, and a new double peak emerged in the visible region with maxima at 510 and 560 nm. As the potential

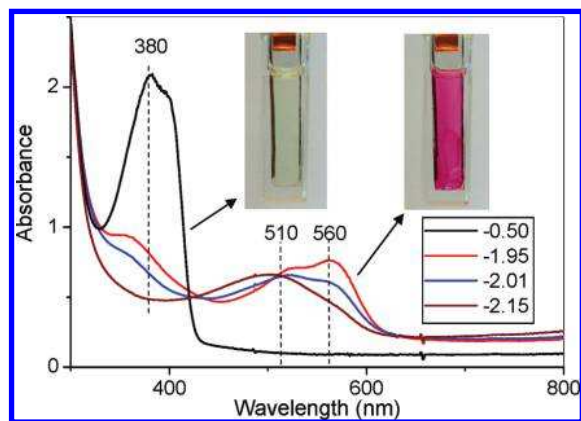


Figure 2. UV-vis spectrum of the PF₄Ox on ITO electrode at different potentials (volts vs Ag quasi-reference electrode).

was decreased to -2.01 V, the absorbance at 560 nm decreased, while the peak at 510 nm remained unchanged. With the potential continuously reduced to -2.15 V, the peak at 560 nm decreased in intensity significantly, at the same time the peak of 510 nm slightly shifted to shorter wavelength with the intensity remaining the same. Referring to the CV data in Figure 1, we can suggest that the peak at 560 nm is associated with the polaron on the Ox-containing segment, and the peak at 510 nm is related to the polaron on the fluorene segment.

As the potential was switched from -0.5 to -1.95 V, the copolymer film changed from colorless to rosy-red. This color stayed when the potential changed between -1.95 and -2.20 V. When potential square-wave cycles ($-0.5 \leftrightarrow -2.01$ V) were applied to the copolymer as shown in Figure 3, the film exhibited a high contrast of the optical transmittance change ($\Delta T\%$) up to 37% and 43% at 510 and 560 nm. The color switching time, defined as the time required for reaching 90% of the full change in absorbance after switching potential, could be estimated from the absorbance profiles, being 1.1 s for coloration and only 1.0 s for bleaching. Figure 3 showed that when the potential on the film was held at -2.01 V, the film transmittance at 560 nm decreased by about 7%, while the transmittance at 510 nm remained unchanged. This change at 560 nm was related to the conversion of the charged states from the red curve to the blue curve in Figure 2. At the initial stage of the potential step at -2.01 V, the polaron of the Ox-containing segment corresponding to the redox couple at -2.06 V would form first; consequently the film showed UV absorption as the red curve in Figure 2. As the formation of this polaron became saturated, the polaron on the fluorene segment corresponding to the redox couple at -2.22 V started to form, and then the UV absorption gradually turned to the blue curve. This conversion resulted in decreased absorption at 560 nm, which became obvious by comparing the intensities of red and blue curves at 560 nm in Figure 2.

Figure 3 also shows a very small change of $\Delta T\%$ with increasing potential square-wave cycling number, indicating high stability of the copolymer film upon electron charging. In 100 cycles, the value of $\Delta T\%$ had only 4.3% decrease at 380 nm and about 9% at 510 and 560 nm. The loss of $\Delta T\%$ in the entire 500 cycles for all peaks is less than 30%.

2. Laser Flash Photolysis. In order to gain additional information on the variation of absorption spectra of the copolymer film under different electrochemical charged states, we conducted a solution laser flash photolysis test for PF₄Ox in benzonitrile in the presence or absence of an electron donor, triethylamine (TEA). The transient absorption spectra recorded

$2.5 \mu\text{s}$ after 355 nm laser excitation of a N₂-purged PF₄Ox solution is shown in Figure 4.

Figure 4 showed a significant change of the transient spectra in the presence or absence of TEA. Particularly, a strong peak appeared at 340 nm when the irradiation was carried out in the presence of TEA, whereas it did not appear in the absence of TEA. An additional test revealed that this peak disappeared again even in the presence of TEA when the solution was purged with oxygen, indicating this peak can be easily quenched by oxygen. It is worth noting that this transient spectrum with a sharp peak at 340 nm is different from the optical spectrum of the electron-charged PF₄Ox recorded in the electrochemical cell at -1.95 V as shown in Figure 2 (red curve). Therefore, we assign this peak to the unrelaxed exciplex of negatively charged PF₄Ox^{•−} polaron with the positive triethylammonium cation. This exciplex was formed by transferring an electron from triethylamine to the excited state of PF₄Ox. The quenching of this peak by oxygen supports this assignment. It is known that oxygen can act as electron acceptor to quench the negatively charged polaron easily.¹¹ The exciplex will be sensitive to the presence of oxygen. Due to the short wavelength of the peak, this transient absorption is believed to correspond mostly to the unrelaxed negative polaron having the charge localized in a single monomer unit where the electron is accepted and strongly interacts with the triethylammonium cation. This unrelaxed negative polaron/triethylammonium exciplex should be able to decay in a longer time period to an equilibrated polaron, whose spectrum should be similar to the one recorded at the electrochemical charged state at -1.95 V as shown in Figure 2 (red curve).

Although the transient spectrum in Figure 4 was recorded at a short delay time of $2.5 \mu\text{s}$, no apparent change of the spectrum was observed in $400 \mu\text{s}$ after the laser pulse, the longest time window available in our nanosecond laser flash system. This phenomenon would indicate that this equilibration was relatively slow. In addition to the observation of the complete oxygen quenching of this localized negative polaron, this phenomenon indicates that when the negative charge is localized in one or a few monomer units, the resulting species is highly vulnerable to the attack of oxygen to cause degradation.

3. Degradation of Copolymer during the Electrochromic Test. It is commonly accepted that the loss of $\Delta T\%$ during the electrochromic cycling of the copolymer film is associated with degradation of the copolymer in the charged state. Most conjugated polymers in the electron-charged state are very reactive and easily react with O₂ or H₂O from the surroundings. A careful examination under an optical microscope of the PF₄Ox film on the ITO electrode before and after the electrochromic test revealed that the film was somewhat damaged after 500 potential square-wave cycles. The film was prepared by dip-coating on a strip of ITO glass ($5 \times 25 \text{ mm}^2$ of coating area), and is about 110 nm thick with a deviation less than 20%. The optical microscopic image of the film in Figure 5A shows the as-prepared film is uniform and contains a few dust particles. After 500 potential square-wave cycles, it can be seen by naked eyes that about 20–30% of the film becomes white with a porous popcorn-like structure, while the other area remains transparent. The optical microscopic image in Figure 5B shows that the “white” area has actually turned to porous structure. But the transparent area is also lightly damaged with the formation of pinholes and uneven reduction of thickness in some areas as indicated by the inhomogeneous color on the film.

The IR spectra of the pristine polymer film, the materials taken from the transparent area and from the porous area, and

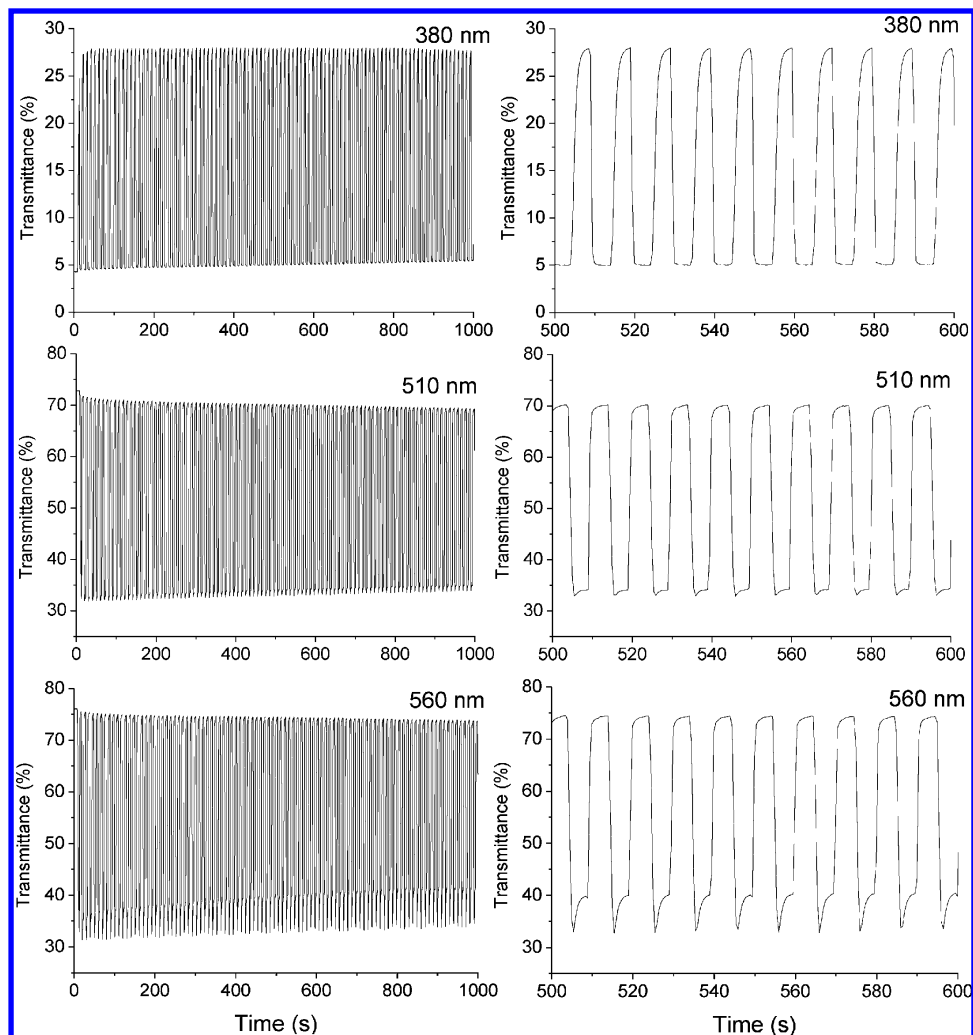


Figure 3. Potential square-wave absorptometry of PF₄Ox in CH₃CN with 0.1 M Bu₄NPF₆ as the supporting electrolyte by applying a potential step (−0.50/−2.01 V) (coated area 5 × 25 mm²) and cycle time 10 s.

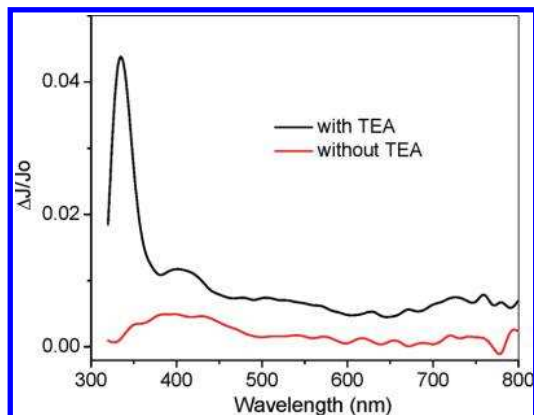


Figure 4. UV-vis transient absorption spectra recorded 2.5 μ s after 355 nm laser excitation of a N₂-purged benzonitrile PF₄Ox solution in the presence and absence of TEA.

the material extracted from the electrolyte solution by toluene were compared in Figure 6. Three characteristic bands were found in the IR spectrum of the pristine polymer film. The band at 2921 and 2841 cm^{-1} is aliphatic C–H stretching mode. The band at 1459 cm^{-1} is attributed to aromatic C=C stretching, and a characteristic band of the PF occurs at 815 cm^{-1} . An additional weak band was developed at 1720 cm^{-1} accompanied with a slightly stronger band at 1677 cm^{-1} in the film after the electrochromic test. The band at 1720 cm^{-1} has been identified

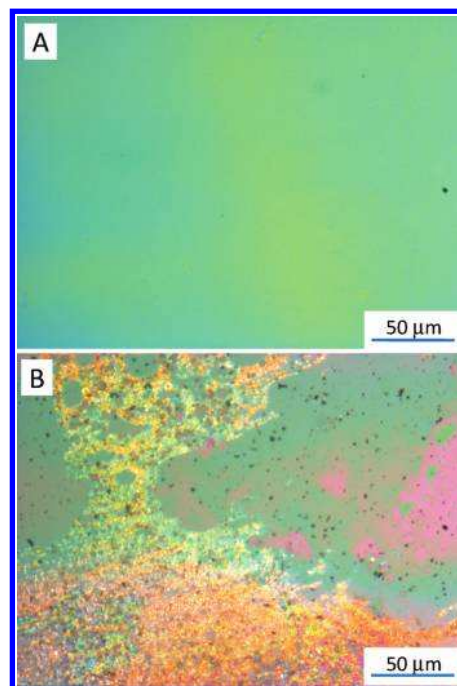


Figure 5. Optical microscopic images of the film on ITO electrode (A) before and (B) after 500 potential square-wave cycles between −0.5 and −2.01 V (vs Ag).

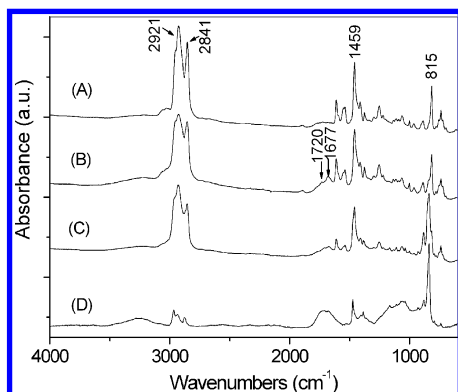


Figure 6. IR spectra of PF₄Ox of (A) the original polymer film and (B–D) after 500 potential square-wave cycles between -0.5 and -2.01 (volts vs Ag): (B) sample from transparent area on electrode; (C) sample from damaged area on electrode; (D) sample extracted from electrolyte solution by toluene.

as the C=O stretching mode of the fluorenone unit in the polymer.¹⁰ It is reported that fluorenone defects could be introduced into the fluorene polymers by photo- or thermochemical processes and by charge injection under the operation of light-emitting devices.^{10,11} It was observed that the IR spectrum of the material from the porous area has a similar intensity of the fluorenone peak as the materials from the transparent area, while the degraded species extracted from the electrolyte solution had a much more pronounced band at 1720 cm^{-1} . This phenomenon indicated that electrochemical degradation of the copolymer produced fluorenone units in the film and some fluorenone-rich fragments were dissolved into the electrolyte solution, leading to the damage of the film. Comparing the IR spectra again in Figure 6 indicates that the aliphatic C–H stretch band of the copolymer after the electrochromic test becomes weaker. This band becomes even much weaker for the degraded material extracted from the solution. This result is consistent with the conclusion of formation of fluorenone defects. As soon as it is formed, the octyl side chain was detached. The position of the peak at 815 cm^{-1} of the copolymer from the transparent area is not apparently affected by the potential square-wave cycling. But this band in the spectrum of the material from the porous area or of the extracted residual is shifted to higher frequency at 833 cm^{-1} , corresponding to the shorter oligofluorene structure containing higher fluorenone content as reported in the literature.^{10a} This result indicates the degradation of the copolymer is more severe in the porous area than the transparent area. On the other hand, another C=O stretching band at a lower frequency of 1677 cm^{-1} has been observed in all the samples after the electrochromic test. This band is attributed to the quinone structures. All the results indicate that the keto defect as well as the quinone defect has been formed during the potential square-wave cycling at the 9-carbon and aromatic carbon of the fluorene unit, respectively.

4. Reversible Inner Peaks Observed in CV Cycling. The stability of the copolymer upon electrochemical reduction and oxidation was re-examined by CV with the copolymer coated on Pt working electrode. As mentioned above, the copolymer film exhibited high stability to the separate multiple n-doping and p-doping scans. A very small current drop with a similar scale as the $\Delta T\%$ drop observed in the potential square-wave cycling has been observed after each scan. However, when the film was CV scanned cyclically over the whole potential range including both the n- and p-doping processes between -2.3 and 1.6 V , a pair of inner peaks emerged along with the main n- and p-doping redox couples. This behavior is demonstrated in

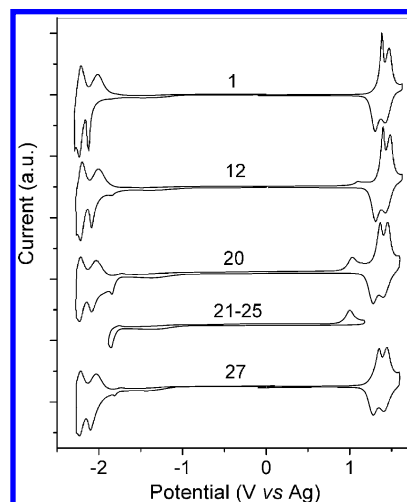


Figure 7. Cyclic voltammograms of the PF₄Ox film, which was drop-coated on Pt disk electrode, and the CV was recorded in $0.1\text{ M Bu}_4\text{NPF}_6$ solution of CH_3CN at a scan rate of 50 mV/s . The potentials are measured relative to an Ag wire quasi-reference electrode. The number above each curve represents the scan number of the curve. The sample was first scanned separately for n- and p-doping (10 cycles each) and then was scanned in the whole range between -2.3 and 1.6 V (cycles 11–20). A pair of inner peaks developed during the wide-range scanning, and it remained unchanged if the sample was scanned only in the inner peaks region (cycles 21–25). The inner peaks disappeared if the scanning was switched back to n- and p-doping processes separately.

Figure 7, where the number above each CV curve represents the scan number. As the test was started with separate scans of the n- and p-doping processes, the CV curves did not show notable change in 10 cycles. Starting from 11th cycle, the copolymer film was scanned over the whole region. In this case, a pair of inner peaks started to appear at -1.84 and 1.03 V . The current associated with these inner peaks gradually increased as the cycling number increased, accompanied with a same-scale current decrease of the main n- and p-doping redox couples, which was more pronounced than the current decrease of the cycles in separate n- and p-doping processes (curves 1–10). When the cycling (cycles 21–25) was carried out in the potential range encompassing only the inner peaks, they remained reversible with their intensity unchanged with cycles. It was also interesting to note that when the CV scans were reverted back to scan n- and p-doping processes separately, the newly formed peaks completely disappeared after only one scan and the shape of the CV curve returned to that observed before the full-range scanning commenced. However, the current of the n- and p-doping was not fully recovered and remained at the same value of the last full-range cycling (cycle 20). The scan in the inner peaks region again produced the same curve as curves 21–25. It should be noted that similar phenomena have been reported for polythiophenes¹² and some other charge-transfer copolymers.¹³ While the origin of this pair of inner peaks is not fully understood, we can find unique characteristics for them; that is, they are a redox couple. The CV curves remain unchanged when the samples are cyclically scanned in this region (cycles 22–25) and disappear when the sample is scanned for n- or p-doping separately. Therefore, we believe that this pair of inner peaks is associated with formation of the keto defect during the electrochemical redox process of the copolymer film.^{10,11} The content of the formed keto defect has increased with the redox cycling process, as indicated by the increased intensity of the inner peaks in cycles 12–20. As soon as the keto defect is formed, it can serve as a charge carrier trap,^{11,14}

which can be quenched only with the opposite charge injection. This property explains the observation of the reversible inner peaks when the sample is scanned in the inner peak region (cycles 22–25). However, if the sample is potential-scanned separately for n- and p-doping processes, the keto defects are saturated by the charge carrier and therefore they act as an inactive site to the CV scan, and then become invisible in cycle 27. This assumption is supported by the similar CV behavior found in the fluorenone-containing polymers.^{14a} An additional Fourier transform infrared (FT-IR) study (not shown) of the sample taken from the Pt working electrode after this series of the CV experiment revealed an IR spectrum similar to Figure 6b, with a slightly weaker absorption band at 1720 cm⁻¹, confirming the formation of fluorenone structure in the copolymer, which acted as a charge trap, led to the formation of the pair of inner peaks, and resulted in a decay of the electrochromic property of the copolymer.

Conclusion

In conclusion, we have reported electrochromic properties of PF₄Ox with high contrast and fast switching from colorless at the neutral state to rosy-red at the electron-charged state. By comparison with the fluorene homopolymer PF, this alternating copolymer of quarter(9,9-dioctylfluorene) and oxadiazole exhibited much higher stability in the electron charging, resulted in a highly stable n-doping electrochromic property. With the electron charging, the film turned from transparent, with an absorption band in the UV region at ~380 nm, to rosy-red, with a strong absorption showing maxima at 510 and 560 nm. The peak at 510 nm corresponds to the polaron on the fluorene segment, while the peak at 560 nm is associated with the polaron on the Ox-containing segment. The potential square-wave cycling of the film produced a high contrast of the color change with $\Delta T\%$ up to 43%. Switching times as short as 1.1 s for coloration and 1.0 s for bleaching were reached. Long time potential square-wave cycling degraded the electrochromic performance. After 500 cycles, about 30% of $\Delta T\%$ value was lost. It is found to be associated with degradation of the copolymer chain by formation of fluorenone and quinone defects in the copolymer. Laser flash photolysis indicated that the localized negative polaron formed instantaneously after the laser pulse and readily reacted with oxygen, leading probably to the formation of the defects. The FT-IR study revealed that these defects were formed in the copolymer during the n-doping electrochromic cycling. A careful CV study of this copolymer also revealed that formation of the defects during the electrochemical redox cycling produced a pair of inner peaks at -1.84 and 1.03 V. They reversibly appeared in the CV curve when the scan completely covered this region, corresponding to the process that the charge carriers were trapped by the keto defect and quenched with the opposite charge injection and vice versa.

Acknowledgment. Financial support by the joint Canadian–Spanish NRC–CSIC program, the NRC–Nano program, and the NRC–NSERC–BDC program is gratefully acknowledged.

References and Notes

- (1) (a) Mortimer, R. G. *Chem. Soc. Rev.* **1997**, 26, 147–156. (b) Sonmez, G. *Chem. Commun.* **2005**, 42, 5251–5259. (c) Argun, A. A.; Aubert, P.-H.; Thompson, B. C.; Schwendeman, I.; Gaupp, C. L.; Hwang, J.; Pinto, N. J.; Tanner, D. B.; MacDiarmid, A. G.; Reynolds, J. R. *Chem. Mater.* **2004**, 16, 4401–4412.
- (2) (a) Somani, P. R.; Radhakrishnan, S. *Mater. Chem. Phys.* **2003**, 77, 117–133. (b) Mortimer, P. J.; Dyer, A. L.; Reynolds, J. R. *Displays* **2006**, 27, 2–18.
- (3) Bange, K.; Bambke, T. *Adv. Mater.* **1990**, 2, 10–16.
- (4) (a) Welsh, D. M.; Kloeppner, L. J.; Madrigal, L.; Pinto, M. R.; Thompson, B. C.; Schanze, K. S.; Abboud, K. A.; Powell, D.; Reynolds, J. R. *Macromolecules* **2002**, 35, 6517–6525. (b) Reeves, B. D.; Grenier, C. R. G.; Argun, A. A.; Cirpan, A.; McCarley, T. D.; Reynolds, J. R. *Macromolecules* **2004**, 37, 7559–7569. (c) Sonmez, G.; Sonmez, H. B.; Shen, C. K. F.; Jost, R. W.; Rubin, Y.; Wudl, F. *Macromolecules* **2005**, 38, 669–675. (d) Sonmez, G.; Sonmez, H. B.; Shen, C. K. F.; Wudl, F. *Adv. Mater.* **2004**, 16, 1905–1908. (e) Sonmez, G.; Shen, C. K. F.; Rubin, Y.; Wudl, F. *Angew. Chem., Int. Ed.* **2004**, 43, 1498–1500.
- (5) (a) Nicho, M. E.; Hu, H.; Lopez-Mata, C.; Escalante, J. *Sol. Energy Mater. Sol. Cells* **2004**, 82, 105–118. (b) Shawn, A.; Sotzing, G. A.; Reynolds, J. R. *Chem. Mater.* **1998**, 10, 2101–2108. (c) Huang, S.-W.; Ho, K.-C. *Sol. Energy Mater. Sol. Cells* **2006**, 90, 491–505. (d) Thompson, B. C.; Schottland, P.; Zong, K.; Reynolds, J. R. *Chem. Mater.* **2000**, 12, 1563–1571.
- (6) (a) Sotzing, G. A.; Reddinger, J. L.; Katritzky, A. R.; Soloducho, J.; Musgrave, R.; Reynolds, J. R. *Chem. Mater.* **1997**, 9, 1578–1587. (b) Beaupre, S.; Dumas, J.; Leclerc, M. *Chem. Mater.* **2006**, 18, 4011–4018. (c) Balan, A.; Gunbas, G.; Durmus, A.; Toppare, L. *Chem. Mater.* **2008**, 20, 7510–7513. (d) Hsiao, S.-H.; Liou, G.-S.; Kung, Y.-C.; Yen, H.-J. *Macromolecules* **2008**, 41, 2800–2808.
- (7) (a) Witker, D.; Reynolds, J. R. *Macromolecules* **2005**, 38, 7636–7644. (b) Galand, E. M.; Mwaura, J. K.; Argun, A. A.; Abboud, K. A.; McCarley, T. D.; Reynolds, J. R. *Macromolecules* **2006**, 39, 7286–7294. (c) Heuer, H. W.; Wehrmann, R.; Kirchmeyer, S. *Adv. Funct. Mater.* **2002**, 12, 89–94.
- (8) (a) Fei, J.; Lim, K. G.; Palmore, G. T. R. *Chem. Mater.* **2008**, 20, 3832–3839. (b) Sonmez, G.; Meng, H.; Wudl, F. *Chem. Mater.* **2004**, 16, 574–580.
- (9) (a) Ding, J.; Day, M.; Robertson, G.; Roovers, J. *Macromolecules* **2002**, 35, 3474–3483. (b) Ding, J.; Tao, Y.; Day, M.; Roovers, J.; D'Iorio, M. *J. Opt. A: Pure Appl. Opt.* **2002**, 4, S267–S272.
- (10) (a) Kulkarni, A. P.; Kong, X.; Jenekhe, S. A. *J. Phys. Chem. B* **2004**, 108, 8689–8701. (b) Panozzo, S.; Vial, J.-C.; Kervella, Y.; Stephan, O. *J. Appl. Phys.* **2002**, 92, 3495–3502. (c) Gong, X.; Iyer, P. K.; Moses, D.; Bazan, G. C.; Heeger, A. J.; Xiao, S. *Adv. Funct. Mater.* **2003**, 13, 325–330. (d) Lee, J. I.; Klaerner, G.; Miller, R. D. *Chem. Mater.* **1999**, 11, 1083–1088.
- (11) (a) List, E. J. W.; Guentner, R.; Scanducci de Freitas, P.; Scherf, U. *Adv. Mater.* **2002**, 14, 374–378. (b) Scherf, U.; List, E. J. W. *Adv. Mater.* **2002**, 14, 477–487.
- (12) (a) Borjas, R.; Buttry, D. A. *Chem. Mater.* **1991**, 3, 872–878. (b) Zotti, G.; Schiavon, G.; Zecchin, S. *Synth. Met.* **1995**, 72, 275–281.
- (13) (a) Yamamoto, T.; Zhou, Z.-H.; Kanbara, T.; Shimura, M.; Kizu, K.; Maruyama, T.; Nakamura, Y.; Fukuda, T.; Lee, B.-L.; Ooba, N.; Tomaru, S.; Kurihara, T.; Kaino, T.; Kubota, K.; Sasaki, S. *J. Am. Chem. Soc.* **1996**, 118, 10389–10399. (b) Lee, B.-L.; Yamamoto, T. *Macromolecules* **1999**, 32, 1375–1382.
- (14) (a) Levi, M. D.; Demadrille, R.; Markevich, E.; Gofer, Y.; Pron, A.; Aurbach, D. *Electrochem. Commun.* **2006**, 8, 993–998. (b) Gong, X.; Moses, D.; Heeger, A. J.; Xiao, S. *J. Phys. Chem. B* **2004**, 108, 8601–8605.

JP9108927